

Surface Analysis

Comparing the Self-Assembly of Sexiphenyl-Dicarbonitrile on Graphite and Graphene on Cu(111)

Nico Schmidt,^[a] Jun Li,^[a] Stefano Gottardi,^[a] Juan Carlos Moreno-Lopez,^[a, f] Mihaela Enache,^[a] Leticia Monjas,^[b] Ramon van der Vlag,^[b] Remco W. A. Havenith,^[a, b, c] Anna K. H. Hirsch,^[b, d, e] and Meike Stöhr^{*[a]}

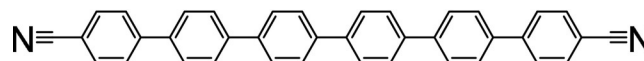
Abstract: A comparative study on the self-assembly of sexiphenyl-dicarbonitrile on highly oriented pyrolytic graphite and single-layer graphene on Cu(111) is presented. Despite an overall low molecule–substrate interaction, the close-

packed structures exhibit a peculiar shift repeating every four to five molecules. This shift has hitherto not been reported for similar systems and is hence a unique feature induced by the graphitic substrates.

Introduction

Graphene as a 2D material with exceptional properties holds great promise in future electronic applications.^[1,2] The introduction of organic molecules can be seen as a way to easily and cheaply steer the already outstanding properties of graphene. Accordingly, molecular self-assembly on graphene has been increasingly studied in the last years.^[3–6] To date, studies almost exclusively observed an influence of the substrate on

molecular self-assemblies when the molecules were deployed on strongly corrugated graphene substrates such as graphene on Ru(0001).^[7–9] On substrates where the interaction of graphene with the underlying metal substrate is weak, e.g., Pt(111), SiC, or Cu(111), the self-assembly was mainly governed by intermolecular interactions.^[10–14]



Scheme 1. Chemical structure of sexiphenyl-dicarbonitrile (NC-Ph₆-CN).

Herein, we report the self-assembly of sexiphenyl-dicarbonitrile (NC-Ph₆-CN, Scheme 1) on highly oriented pyrolytic graphite (HOPG) and single-layer graphene on Cu(111). We studied the structural and electronic properties of the molecules using scanning tunneling microscopy (STM), scanning tunneling spectroscopy (STS), and low-energy electron diffraction (LEED).

Complementary information was obtained from density functional theory (DFT) calculations. For NC-Ph₆-CN on HOPG, we found a close-packed structure in which parallel molecules align in rows. A peculiar feature was a shift of every fourth molecule. Such a shift has not previously been reported for similar molecules on metallic substrates or for the bulk crystal.^[15,16] Upon deposition of NC-Ph₆-CN on graphene on Cu(111), we found two related close-packed structures. In both structures, the parallel molecules again aligned in rows with molecules shifting either every fourth or fifth molecule. This indicates that: 1) the observed shift is per se a unique feature of NC-Ph₆-CN on graphitic substrates and 2) one layer of graphene already suffices to induce it. Furthermore, we could identify small but distinct differences in the NC-Ph₆-CN structures on HOPG compared with single-layer graphene on Cu(111), demonstrating that even for weakly corrugated graphene substrates the role of the underlying metal substrate is not negligible.

[a] N. Schmidt, Dr. J. Li, Dr. S. Gottardi, Dr. J. C. Moreno-Lopez, Dr. M. Enache, Dr. R. W. A. Havenith, Prof. Dr. M. Stöhr
Zernike Institute for Advanced Materials
University of Groningen, Nijenborgh 4
9747 AG Groningen (The Netherlands)
E-mail: m.a.stoehr@rug.nl

[b] Dr. L. Monjas, R. van der Vlag, Dr. R. W. A. Havenith, Prof. Dr. A. K. H. Hirsch
Stratingh Institute for Chemistry
University of Groningen, Nijenborgh 7
9747 AG Groningen (The Netherlands)

[c] Dr. R. W. A. Havenith
Ghent Quantum Chemistry Group
Department of Inorganic and Physical Chemistry
Ghent University, Krijgslaan 281 (S3), 9000 Ghent (Belgium)

[d] Prof. Dr. A. K. H. Hirsch
Department of Drug Design and Optimization (DDOP)
Helmholtz Institute for Pharmaceutical Research Saarland
66123 Saarbrücken (Germany)

[e] Prof. Dr. A. K. H. Hirsch
Department of Pharmacy, Saarland University
Campus Building E8.1, 66123 Saarbrücken (Germany)

[f] Dr. J. C. Moreno-Lopez
Current affiliation: Faculty of Physics
University of Vienna, Strudlhofgasse 4, 1090 Vienna (Austria)

Supporting information and the ORCID identification number(s) for the author(s) of this article can be found under:
<https://doi.org/10.1002/chem.201806312>.

© 2019 The Authors. Published by Wiley-VCH Verlag GmbH & Co. KGaA. This is an open access article under the terms of Creative Commons Attribution NonCommercial License, which permits use, distribution and reproduction in any medium, provided the original work is properly cited and is not used for commercial purposes.

Results and Discussion

NC-Ph₆-CN on HOPG

After deposition of a submonolayer coverage of NC-Ph₆-CN onto HOPG, we performed STM measurements at 5 K. This temperature was necessary to restrict molecular movement observed at higher temperatures. We found NC-Ph₆-CN assembled into a close-packed structure exhibiting long-range order with island sizes of several hundred nanometers. However, we observed a considerable number of defects (Figure S1a). An overview STM image of NC-Ph₆-CN on HOPG is shown in Figure 1a. The molecules assembled into parallel rows as indicated by grey lines. A high-resolution STM image (Figure 1b) reveals the molecular assembly in detail. Individual molecules can be discerned as rod-shaped protrusions. Black lines representing individual molecules are added in the image to guide the eye. Within one row, the molecules are parallel to each other. Furthermore, each fourth molecule along a row was shifted along the long axis of the molecules. Based on this peculiar feature, we determined the oblique unit cell of NC-Ph₆-CN on HOPG (marked in green) as $a = 2.9$ nm, $b = 2.2$ nm, $\theta = 104^\circ$.

Figure 1c shows a tentative structural model of NC-Ph₆-CN on HOPG. The unit cell contains three molecules. Every fourth

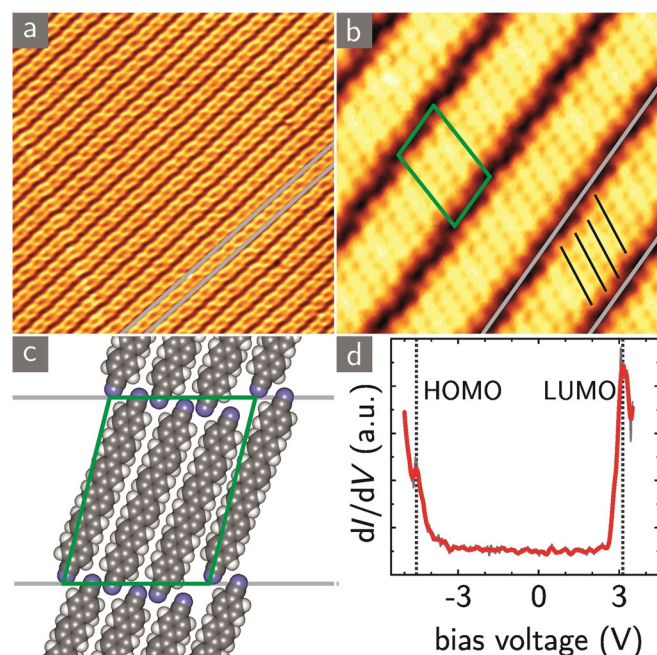


Figure 1. Self-assembly and electronic structure of NC-Ph₆-CN on HOPG. a) Overview STM image (50×50 nm², 3.2 V, 8 pA, 5 K). The molecules are arranged into a close-packed structure consisting of parallel rows. Grey lines highlight one row. b) High-resolution STM image (10×10 nm², 2.8 V, 3 pA, 5 K). The oblique unit cell of the structure is shown in green. Black lines indicate individual molecules. One row is highlighted by grey lines. c) Tentative structural model. The unit cell contains three molecules. Every fourth molecule within a row exhibits a shift. d) STS spectrum of a NC-Ph₆-CN molecule ($U_{\text{set}} = 3.5$ mV, $I_{\text{set}} = 150$ pA). The spectrum was taken in the center of the molecule. The dotted lines denote the HOMO level at -4.6 V and the LUMO level at 3.1 V, respectively.

molecule within a row is shifted by approximately one phenyl ring along the long axis of the molecule. Looking from one row to the other, we see that molecules are positioned in such a way that opposing carbonitrile groups interdigitate. Such a formation of antiparallel, interdigitating carbonitrile groups was reported to be the most stable structure for benzonitrile molecules in the gas phase and on Au(111), and has also been seen for NC-Ph₆-CN on Ag(111).^[16,17] We therefore propose that the following intermolecular interactions stabilized the close-packed structure of NC-Ph₆-CN on HOPG: 1) dipolar coupling between opposing carbonitrile groups and 2) H-bonding (CN \cdots HC) between the CN group of one molecule and the closest CH of the opposing molecule.

We would like to point out that, under certain tip conditions, the molecules exhibited a zigzag shape (Figure S1b). This shape is a fingerprint of alternately twisted phenyl rings and was reported for *para*-sexiphenyl (Ph₆) as well as for NC-Ph₆-CN on Ag(111).^[15,18] Near-edge X-ray absorption fine-structure measurements of NC-Ph₆-CN on Ag(111) was used to determine the twisting angle as $\delta = \pm 25^\circ$ with respect to the molecular plane.^[15] As we cannot quantify the twisting angle for NC-Ph₆-CN on HOPG, we used the angle of $\delta = \pm 25^\circ$ for our structural model (Figure 1c). It should be noted that the zigzag shape for NC-Ph₆-CN on Ag(111) was only reported for a second layer of molecules. The first layer of NC-Ph₆-CN did not show a zigzag shape because of the interaction with the metal substrate. In our case, the interaction of NC-Ph₆-CN with HOPG was consequently small enough to promote a zigzag contrast in STM already for the first layer of molecules.

To further investigate the molecule–substrate interactions, we probed the electronic structure of NC-Ph₆-CN on HOPG using STS. Figure 1d shows a STS spectrum taken on top of a NC-Ph₆-CN molecule in the close-packed structure. Two peaks at -4.6 V and 3.1 V can be seen. We attribute these to the highest occupied and lowest unoccupied molecular orbital (HOMO and LUMO) of NC-Ph₆-CN on HOPG, respectively. This leads to a large band gap of $E_{\text{gap}} = 7.7$ eV, suggesting that NC-Ph₆-CN interacts only weakly with the underlying HOPG. Together with the observed alternating twisting of the phenyl rings, we conclude that NC-Ph₆-CN is physisorbed on HOPG.

One outstanding feature of the close-packed structure of NC-Ph₆-CN on HOPG is the shift of every fourth molecule along a row. Such a feature has not been observed on metallic substrates. To further investigate this shift, the self-assembly of NC-Ph₆-CN on graphene on Cu(111) was studied. By moving from multilayer to single-layer graphene, we reduce the number of graphene sheets to the ultimate limit of one. By doing so, we address the questions of whether a single layer of graphene suffices to induce this peculiar shift and which, if any, influence the underlying Cu(111) has on the molecular self-assembly.

NC-Ph₆-CN on graphene on Cu(111)

Upon deposition of submonolayer coverage of NC-Ph₆-CN onto graphene on Cu(111), we were able to perform STM measurements at 77 K, indicating an increased diffusion barrier

compared with HOPG. We again observed a close-packed structure with exceptional long-range order. In contrast to the case of HOPG, the molecular islands showed fewer defects on graphene on Cu(111) (Figure S1c). We attribute this to the higher structural quality of epitaxially grown graphene compared with mechanically cleaved HOPG, that is, the lack of well-known large-scale morphological deviation in HOPG derived from mechanical cleavage.^[19]

A close look at NC-Ph₆-CN on graphene on Cu(111) revealed that there were, in fact, two phases of close-packed structure. Both phases are shown in Figure 2a and Figure 2b, respectively. In both images, individual molecules can be identified as rod-shaped protrusions. Black lines representing individual molecules are added to the image to guide the eye. Similar to the case of NC-Ph₆-CN on HOPG, the molecules assembled for both phases into rows, as indicated by the grey lines. For both phases, we observed a shift similar to that of NC-Ph₆-CN on HOPG. However, the difference between the two phases lies in the frequency of the aforementioned shift. In phase 1 (Figure 2a, marked in cyan), every fourth molecule along a row was shifted. In phase 2 (Figure 2b, marked in magenta), this shift occurred only every fifth molecule along a row. Accordingly, the unit cells differ in size. For phase 1, we determined an oblique unit cell with $a_1=2.9$ nm, $b_1=2.2$ nm, $\Theta_1=94^\circ$ while the oblique unit cell of phase 2 has the values $a_2=2.9$ nm, $b_2=2.6$ nm, $\Theta_2=106^\circ$. Figure 2c shows a tentative structural model of phase 1. The unit cell of phase 1 contains

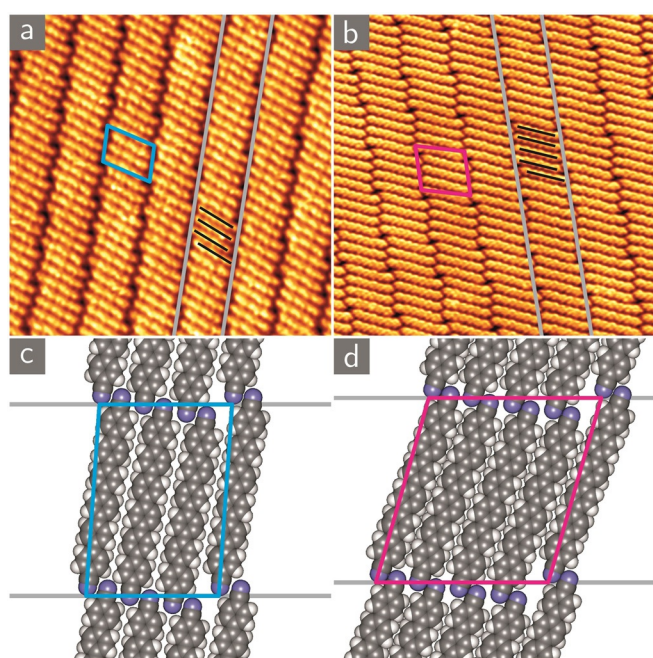


Figure 2. Self-assembly of NC-Ph₆-CN on graphene on Cu(111). a) High-resolution STM image of phase 1 (20×20 nm², 1.2 V, 20 pA, 77 K). The oblique unit cell is shown in cyan. One row of molecules is highlighted by grey lines. Black lines indicate individual molecules. b) High-resolution STM image of phase 2 (20×20 nm², -1.6 V, 20 pA, 77 K).^[55] The oblique unit cell is shown in magenta. c) Tentative structural model of phase 1. The unit cell of phase 1 contains three molecules. Every fourth molecule within a row exhibits a shift. d) Tentative structural model of phase 2. The unit cell of phase 2 contains four molecules. Every fifth molecule within a row exhibits a shift.

three molecules. Similar to the case of NC-Ph₆-CN on HOPG, every fourth molecule within a row exhibits a shift along the long axis of the molecule by approximately one phenyl ring. In contrast, the unit cell of phase 2 contains four molecules (Figure 2d) and every fifth molecule displays a shift. For both phases, the carbonitrile groups of adjacent rows interdigitate. This suggests that, again, a combination of dipolar coupling of opposing carbonitrile groups and H-bonding between CN groups and closest CH groups stabilizes adjacent rows of both phases. We also observed a twisting of the phenyl rings for NC-Ph₆-CN on graphene on Cu(111) (Figure S1d), which was incorporated in the tentative structural models.

To further assess the self-assembly of NC-Ph₆-CN on graphene on Cu(111), we performed LEED measurements.^[20] Graphene epitaxially grown on Cu(111) exhibits multiple rotational domains.^[21] This leads to a ring structure in LEED images that surrounds the diffraction spots of the Cu(111) substrate (Figure S2a). This ring structure has a varying intensity, indicating preferred rotational orientations of graphene on Cu(111). Upon deposition of submonolayer coverage of NC-Ph₆-CN, we noted clear diffraction spots (Figure S2b). Superimposing the simulated LEED patterns for phase 1 and 2 (Figure S2c) yielded good agreement with the observed diffraction spots. Note that for both phases the diffraction spots associated with the long unit cell vector coincided with the [1-10] direction of Cu(111). For almost all STM images, we furthermore found the long unit cell vectors aligned with the direction of the graphene lattice. If we also consider that most graphene domains on Cu(111) are not rotated, this suggests that submonolayer coverages of NC-Ph₆-CN molecules grew preferentially on graphene domains that were not rotated with respect to the underlying Cu(111) surface lattice.

Computational Results

To gain additional insight into the behavior of NC-Ph₆-CN, we performed DFT calculations. In a first step, we aimed to calculate the band gap by studying the individual molecule in the gas phase. However, when compared to the experimentally determined value of $E_{\text{gap}}=7.7$ eV, the most commonly used functionals for similar systems failed to reproduce the experimentally determined band gap for NC-Ph₆-CN (Table S1). Even more sophisticated functionals (e.g., optimally tuned range-separated hybrid functionals such as HSE) failed to describe the system. Only by tuning the fraction of the Hartree-Fock (HF) exchange was a calculated value of the band gap closer to the experimental one obtained (Figure 3a and Table S1). By using the PBE0 hybrid exchange-correlation functional (which has a 25% HF exchange contribution)^[22,23] with dispersion corrections included,^[24] a band gap of 4.23 eV for NC-Ph₆-CN was obtained. Our situation is similar to, for example, the case of benzene, for which a band gap of 10.3 eV was determined experimentally, while the calculated value was ca. 5 eV.^[25] This so-called “band gap problem” is well known in the theoretical modeling community.^[26] However, it should be noted that a discrepancy between calculated band gap and STS measure-

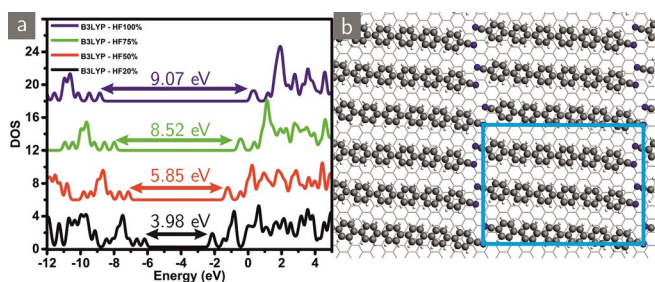


Figure 3. Computational results for NC-Ph₆-CN. a) DFT gas-phase calculations for NC-Ph₆-CN using a hybrid functional^[51] and varying its Hartree–Fock (HF) exchange contribution.^[52] With increasing the HF exchange contribution the density of states of NC-Ph₆-CN exhibits an increasing band gap. The spectra are offset for better visualization. b) NC-Ph₆-CN adsorbed on graphene. The unit cell is marked in cyan.

ments could also be the result of temporary charging of the molecule^[27] facilitated by a double barrier tunnel junction.^[28,29]

In a second step, we looked at the adsorption of NC-Ph₆-CN on graphene by comparing an individually adsorbed molecule, a unit cell without shift, and a unit cell that incorporates a shift every fourth molecule (Figure S3).^[30] Without shift, we determined a unit cell of $a = 2.9$ nm, $b = 0.7$ nm, $\theta = 90^\circ$. The unit cell with shift of every fourth molecule was $a = 2.9$ nm, $b = 2.2$ nm, $\theta = 90^\circ$ (Figure 3b), agreeing reasonably well with our experimental values. Comparing the adsorption energies (Table S2), we find an energy gain of 0.07 eV per molecule in the unit cell with shift compared with the unit cell without shift. This means that the incorporation of a shift is slightly energetically favorable on graphene. It should be noted that the shifted unit cell did not converge during gas-phase calculations, that is, the presence of the graphitic substrate was a prerequisite for the emergence of the shift.

Discussion

At this point, we would like to address the previously posed question and highlight the changes to the molecular assembly of NC-Ph₆-CN when replacing the HOPG substrate with graphene on Cu(111). Although Cu(111) is regarded as weakly interacting with graphene,^[31] we observed several aspects indicating an increased diffusion barrier and molecule–substrate interaction in comparison to HOPG: 1) we were able to perform STM measurements at 77 K and found stable molecular structures. A fortiori, LEED measurements showed that these structures were even stable at RT. In contrast, NC-Ph₆-CN on HOPG could only be imaged in STM when cooled to 5 K and was mobile at higher temperatures. 2) On HOPG, the NC-Ph₆-CN close-packed structure exhibited a shift with every fourth molecule along a row. On graphene on Cu(111), we observed two phases with a shift every fourth and every fifth molecule, respectively. While the shift remained upon moving from multilayer to single-layer graphene, the presence of the underlying metal substrate for single-layer graphene facilitated the existence of a second, distinct phase. 3) STM showed both phases of NC-Ph₆-CN on graphene on Cu(111) aligned with the graphene lattice. LEED data showed that both phases coincided

with the [1-10] direction of Cu(111). This suggests a preferential growth of both phases on graphene domains that were not rotated with respect to the Cu(111) lattice. On HOPG, in contrast, we did not observe a preferred orientation of the close-packed structure with respect to the underlying substrate lattice in STM. Furthermore, we were not able to perform LEED measurements of NC-Ph₆-CN on HOPG. This indicates that the molecules were mobile at RT and that the diffusion barrier was considerably smaller on HOPG compared with graphene on Cu(111). All these points are indicative of an increased diffusion barrier and molecule–substrate interaction for NC-Ph₆-CN on graphene on Cu(111) compared with HOPG. It should be noted that the lattice contraction of graphene on Cu(111)^[53,54] could be another reason for the aforementioned differences of the structures. Now we would like to focus on the most peculiar feature of the close-packed structure of NC-Ph₆-CN on HOPG and on graphene on Cu(111)—the occurrence of a shift every fourth or fifth molecule. We start by highlighting previous investigations on similar molecules or substrates. Submonolayer coverages of the unfunctionalized parent molecule of NC-Ph₆-CN, *para*-sexiphenyl (Ph₆), assembled into a close-packed structure of flat-lying, parallel molecules arranged in rows on Au(111), HOPG, and single-layer graphene on Ir(111).^[32–34] Increasing the coverages led to Ph₆ molecules adsorbed with their edge facing the substrate. By introducing terminal carbonitrile groups, Kühne et al. observed structural changes of the close-packed structure of NC-Ph₆-CN on Ag(111) in comparison to Ph₆.^[16] For coverages below 0.5 ML, NC-Ph₆-CN on Ag(111) assembled into a variety of coexisting structures. For coverages close to one monolayer, NC-Ph₆-CN on Ag(111) again formed rows of parallel molecules. Within the rows, the molecules were densely packed while the interdigitating carbonitrile groups connected one row to another. Contrasting this to our observations for graphitic substrates, we can recognize two key differences: 1) we found the same structures independent of coverage. 2) While the close-packed structure of NC-Ph₆-CN on Ag(111) is similar to the structures found by us, most noticeably no shift along the long molecular axis was observed on Ag(111). At this point, one may argue that graphene or HOPG are so weakly interacting with NC-Ph₆-CN that intermolecular interactions are driving the observed shift. In this case, the shift should be adopted in the bulk crystal. However, X-ray structure analyses of Ph₆ and NC-Ph₄-CN showed no features resembling a shift.^[15,32] The comparison with the bulk arrangement performed here is warranted, given that it has been reported that 2D molecular self-assembly on surfaces can be similar to the arrangement of the molecules within a certain crystallographic plane in the bulk, especially for weakly interacting surfaces.^[56–59]

From the points made in the previous paragraph, we conclude that the shift observed by us is a result not only of the presence of the dicyanitrile groups but also of the graphitic substrates. Indeed, our DFT calculations indicate that the incorporation of a shift on graphene results in a net gain of energy for the assembly. However, it should be noted that although the adsorption energies are quite similar, no structure without shift was observed on graphene. Hence, we propose that an

additional effect might influence the occurrence of a shift. In comparison to metal substrates, screening effects by graphene's electrons have been shown to, for example, facilitate an otherwise repulsively interacting close-packed structure of F_4TCNQ molecules and to have an exceptionally large screening length on the order of nanometers found for individual charged adsorbates.^[35,36] The shift every fourth or fifth molecule within a row might hence be a unique feature of NC-Ph₆-CN on graphene and HOPG, enabled not only by an energy gain but also by the different screening properties of graphitic substrates compared with metals. We suggest that the incorporation of the shift in the close-packed structures counterbalances the otherwise anisotropic charge distribution due to the linear arrangement of the carbonitrile groups and, consequently, results in a lowering of the overall energy. Given that this tendency to counterbalance an anisotropic charge distribution is expected to be universal, we suggest that similar molecules bearing polar functional groups, such as in our case the carbonitrile group, will also exhibit an altered molecular arrangement on graphene compared with metal substrates.

Conclusion

We observed upon deposition of submonolayer coverage of NC-Ph₆-CN on HOPG a close-packed structure consisting of rows of parallel molecules with a peculiar shift along the molecular long axis of every fourth molecule within a row. The molecule-substrate interaction is weak, as evidenced by the large HOMO-LUMO gap. Depositing NC-Ph₆-CN on graphene on Cu(111) resulted in subtle but distinct changes to the molecular assembly due to the presence of the underlying metal surface. An overall increased molecule-substrate interaction as well as diffusion barrier could be determined while we still observed a shift for every fourth or fifth molecule along a row. Such distinguishing feature has not previously been reported for similar molecules on metallic substrates or in the bulk phase. Furthermore, our calculations show that the presence of the graphene substrate is necessary to observe the incorporation of a shift into the molecular assembly. We conclude that the shift of every fourth or fifth molecule within a row by approximately one phenyl ring is a unique feature of NC-Ph₆-CN on graphitic substrates, possibly additionally promoted by the screening properties of the electrons in the graphene lattice.

Experimental Section

Sample preparation: HOPG was prepared by cleavage under ambient conditions using adhesive tape. A single layer of graphene on Cu(111) was grown ex situ via chemical vapor deposition in a commercial heater (Carbolite). For the graphene growth, the Cu(111) crystal was held at 1280 K in a gas atmosphere of 0.1 mbar Ar and 0.5 mbar H₂ for 4 h. This was followed by additionally introducing 0.5 mbar CH₄ for 5 min. Subsequently, the CH₄ inlet was closed and the sample was kept at 1280 K for an additional 30 min.

After the ex situ sample preparation, both substrates were introduced into an ultra-high vacuum (UHV) chamber with a base pres-

sure of $<1 \times 10^{-10}$ mbar and annealed in situ for 30 min to ensure clean surfaces. The annealing temperatures were 370 K for HOPG and 720 K for graphene on Cu(111).^[37] Subsequently, we sublimed the NC-Ph₆-CN at a temperature of 620 K using a Knudsen cell evaporator (Omnivac). During deposition, the sample was held at room temperature (RT). We define a monolayer (ML) of molecules as the coverage at which the substrate is fully covered by the close-packed structure of NC-Ph₆-CN.

STM and LEED measurements: We performed experiments in a two-chamber UHV setup. The first chamber was equipped with a low-temperature STM (Scienta Omicron GmbH) and had a base pressure $<5 \times 10^{-11}$ mbar. The second chamber hosted a MCP-LEED (Scienta Omicron GmbH) and the Knudsen cell evaporator. The base pressure of the second chamber was $<1 \times 10^{-10}$ mbar. STM and STS measurements were performed at 5 K for HOPG and 77 K for graphene on Cu(111). In contrast, the samples were held at RT for LEED measurements. STM images were obtained in constant current mode using tips made from a mechanically cut Pt/Ir wire. The STS data were acquired with a lock-in using a frequency of 680 Hz and a modulation voltage of 10 mV (rms). All voltages are given with respect to a grounded tip. We processed the STM images using the software WSxM.^[38]

Computational details: The Amsterdam Density Functional (ADF) software package was employed to perform DFT calculations for the single NC-Ph₆-CN molecule in gas phase optimized with different functionals (see the Supporting Information).^[39-41] The BAND software was employed for calculations of the NC-Ph₆-CN molecule on graphene.^[42-46] The numerical integration was performed using the procedure developed by Becke et al.^[47] The triple- ξ with one polarization function (TZP) basis set was used for all calculations. The core-shells of all elements were treated by the frozen-(large)-core approximation.^[48] For all the calculations of NC-Ph₆-CN on graphene the PBE-D3 functional^[49,50] was used and the positions of the carbon atoms within the graphene layer were kept fixed. All the calculations were performed with *k*-space sampling restricted to the Γ -point.

Acknowledgements

We gratefully acknowledge financial support from the Foundation for Fundamental Research on Matter (FOM), part of the Netherlands Organization for Scientific Research (NWO), by NWO (Vidi grant 723.014.008), the European Research Council (ERC-2012-StG 307760-SURFPRO) and the Zernike Institute for Advanced Materials of the University of Groningen. We would like to thank the Center for Information Technology of the University of Groningen for their support and for providing access to the Peregrine high-performance computing cluster. We would like to thank the Berendsen Center for Multiscale Modeling and Material Design of the Zernike Institute for Advanced Materials at the University of Groningen for their support and for providing access to the Nieuwpoort high-performance computing cluster.

Conflict of interest

The authors declare no conflict of interest.

Keywords: graphene · nanostructures · scanning probe microscopy · self-assembly · surface analysis

- [1] K. S. Novoselov, V. I. Fal'ko, L. Colombo, P. R. Gellert, M. G. Schwab, K. Kim, *Nature* **2012**, *490*, 192–200.
- [2] A. C. Ferrari, F. Bonaccorso, V. Fal'ko, K. S. Novoselov, S. Roche, P. Boggioli, S. Borini, F. H. L. Koppens, V. Palermo, N. Pugno, J. A. Garrido, R. Sordan, A. Bianco, L. Ballerini, M. Prato, E. Lidorikis, J. Kivioja, C. Marinelli, T. Ryhanen, A. Morpurgo, J. N. Coleman, V. Nicolosi, L. Colombo, A. Fert, M. Garcia-Hernandez, A. Bachtold, G. F. Schneider, F. Guinea, C. Dekker, M. Barbone, Z. Sun, C. Galiotis, A. N. Grigorenko, G. Konstantatos, A. Kis, M. Katsnelson, L. Vandersypen, A. Loiseau, V. Morandi, D. Neumaier, E. Treossi, V. Pellegrini, M. Polini, A. Tredicucci, G. M. Williams, B. H. Hong, J.-H. Ahn, J. M. Kim, H. Zirath, B. J. van Wees, H. van der Zant, L. Occhipinti, A. Di Matteo, I. A. Kinloch, T. Seyller, E. Quesnel, X. Feng, K. Teo, N. Rupesinghe, P. Hakonen, S. R. T. Neil, Q. Tannock, T. Lofwander, J. Kinaret, *Nanoscale* **2015**, *7*, 4598–4810.
- [3] N. Schmidt, M. Stöhr in *Encycl. Interfacial Chem. Surf. Sci. Electrochem.* (Ed.: K. Wandelt), Elsevier, **2018**, pp. 110–119.
- [4] K. S. Mali, J. Greenwood, J. Adisojoso, R. Phillipson, S. De Feyter, *Nanoscale* **2015**, *7*, 1566–1585.
- [5] J. M. Macleod, F. Rosei, *Small* **2014**, *10*, 1038–1049.
- [6] A. Kumar, K. Banerjee, P. Liljeroth, *Nanotechnology* **2017**, *28*, 082001.
- [7] D. Maccariello, M. Garnica, M. A. Niño, C. Navío, P. Perna, S. Barja, A. L. V. De Parga, R. Miranda, *Chem. Mater.* **2014**, *26*, 2883–2890.
- [8] M. Roos, B. Uhl, D. Künzel, H. E. Hoster, A. Groß, R. J. Behm, *Beilstein J. Nanotechnol.* **2011**, *2*, 365–373.
- [9] Z. X. Zhang, H. L. Huang, X. M. Yang, L. Zang, *J. Phys. Chem. Lett.* **2011**, *2*, 2897–2905.
- [10] A. J. Martínez-Galera, J. M. Gómez-Rodríguez, *J. Phys. Chem. C* **2011**, *115*, 23036–23042.
- [11] Q. H. Wang, M. C. Hersam, *Nat. Chem.* **2009**, *1*, 206–211.
- [12] H. Huang, S. Chen, X. Gao, W. Chen, A. T. S. Wee, *ACS Nano* **2009**, *3*, 3431–3436.
- [13] A. J. Martínez-Galera, N. Nicoara, J. I. Martínez, Y. J. Dappe, J. Ortega, J. M. Gómez-Rodríguez, *J. Phys. Chem. C* **2014**, *118*, 12782–12788.
- [14] J. Li, S. Gottardi, L. Soliany, J. C. Moreno-López, M. Stöhr, *J. Phys. Chem. C* **2016**, *120*, 18093–18098.
- [15] F. Klappenberger, D. Kühne, M. Marschall, S. Neppi, W. Krenner, A. Nefedov, T. Strunskus, K. Fink, C. Wöll, S. Klyatskaya, O. Fuhr, M. Ruben, J. V. Barth, *Adv. Funct. Mater.* **2011**, *21*, 1631–1642.
- [16] D. Kühne, F. Klappenberger, R. Decker, U. Schlickum, H. Brune, S. Klyatskaya, M. Ruben, J. V. Barth, *J. Phys. Chem. C* **2009**, *113*, 17851–17859.
- [17] Y. Okuno, T. Yokoyama, S. Yokoyama, T. Kamikado, S. Mashiko, *J. Am. Chem. Soc.* **2002**, *124*, 7218–7225.
- [18] K. Braun, S. Hla, *Nano Lett.* **2005**, *5*, 73–76.
- [19] H. Chang, A. J. Bard, *Langmuir* **1991**, *7*, 1143–1153.
- [20] Mobility of the molecules on HOPG at temperatures of 77 K and higher prevented the observation of LEED patterns for HOPG samples.
- [21] S. Gottardi, K. Müller, L. Bignardi, J. C. Moreno-López, T. A. Pham, O. Ivashenko, M. Yablonskikh, A. Barinov, J. Björk, P. Rudolf, M. Stohr, *Nano Lett.* **2015**, *15*, 917–922.
- [22] S. Grimme, *J. Comput. Chem.* **2004**, *25*, 1463–1473.
- [23] M. Ernzerhof, G. E. Scuseria, *J. Chem. Phys.* **1999**, *110*, 5029–5036.
- [24] S. N. Steinmann, C. Corminboeuf, *J. Chem. Theory Comput.* **2011**, *7*, 3567–3577.
- [25] F. Flores, J. Ortega, H. Vázquez, *Phys. Chem. Chem. Phys.* **2009**, *11*, 8658–8675.
- [26] L. Kronik, T. Stein, S. Refaely-Abramson, R. Baer, *J. Chem. Theory Comput.* **2012**, *8*, 1515.
- [27] K. Banerjee, A. Kumar, F. F. Canova, S. Kezilebieke, A. S. Foster, P. Liljeroth, *J. Phys. Chem. C* **2016**, *120*, 8772–8780.
- [28] I. Fernández-Torrente, D. Kreikemeyer-Lorenzo, A. Strózecka, K. J. Franke, J. I. Pascual, *Phys. Rev. Lett.* **2012**, *108*, 036801.
- [29] P. Järvinen, S. K. Hämmäläinen, M. Ijäs, A. Harju, P. Liljeroth, *J. Phys. Chem. C* **2014**, *118*, 13320–13325.
- [30] Due to extensive computational costs, we had to forgo a unit cell with the shift every fifth molecule.
- [31] M. Batzill, *Surf. Sci. Rep.* **2012**, *67*, 83–115.
- [32] S. Müllegger, A. Winkler, *Surf. Sci.* **2006**, *600*, 1290–1299.
- [33] Z. H. Wang, K. Kanai, K. Iketaki, Y. Ouchi, K. Seki, *Thin Solid Films* **2008**, *516*, 2711–2715.
- [34] G. Hlawacek, F. S. Khokhar, R. Van Gastel, B. Poelsema, C. Teichert, *Nano Lett.* **2011**, *11*, 333–337.
- [35] H. Z. Tsai, A. A. Omrani, S. Coh, H. Oh, S. Wickenburg, Y. W. Son, D. Wong, A. Riss, H. S. Jung, G. D. Nguyen, G. F. Rodgers, A. S. Aikawa, T. Taniguchi, K. Watanabe, A. Zettl, S. G. Louie, J. Lu, M. L. Cohen, M. F. Crommie, *ACS Nano* **2015**, *9*, 12168–12173.
- [36] D. Wong, F. Corsetti, Y. Wang, V. W. Brar, H.-Z. Tsai, Q. Wu, R. K. Kawakami, A. Zettl, A. A. Mostofi, J. Lischner, M. F. Crommie, *Phys. Rev. B* **2017**, *95*, 205419.
- [37] The difference in temperature arises from technical restrictions. Cu(111) crystals were mounted on sample holders using clamps whereas HOPG crystals had to be glued on. The limitations of the glue resulted in lower annealing temperature for HOPG.
- [38] I. Horcas, R. Fernández, J. M. Gómez-Rodríguez, J. Colchero, J. Gómez-Herrero, A. M. Baro, *Rev. Sci. Instrum.* **2007**, *78*, 013705.
- [39] G. Te Velde, F. M. Bickelhaupt, E. J. Baerends, C. F. Guerra, S. J. A. van Gisbergen, J. G. Snijders, T. Ziegler, *J. Comput. Chem.* **2001**, *22*, 931–967.
- [40] C. F. Guerra, J. G. Snijders, G. te Velde, E. J. Baerends, *Theor. Chem. Acc.* **1998**, *99*, 391–403.
- [41] ADF2017, SCM, Theoretical Chemistry, Vrije Universiteit, Amsterdam, The Netherlands, <https://www.scm.com>.
- [42] G. Te Velde, E. J. Baerends, *Phys. Rev. B* **1991**, *44*, 7888–7903.
- [43] G. Wiesenekker, E. J. Baerends, *J. Phys. Condens. Matter* **1991**, *3*, 6721–6742.
- [44] M. Franchini, P. H. T. Philipsen, L. Visscher, *J. Comput. Chem.* **2013**, *34*, 1819–1827.
- [45] M. Franchini, P. H. T. Philipsen, E. Van Lenthe, L. Visscher, *J. Chem. Theory Comput.* **2014**, *10*, 1994–2004.
- [46] BAND2017, SCM, Theoretical Chemistry, Vrije Universiteit, Amsterdam, The Netherlands, <http://www.scm.com>.
- [47] A. D. Becke, *J. Chem. Phys.* **1988**, *88*, 2547–2553.
- [48] E. J. Baerends, D. E. Ellis, P. Ros, *Chem. Phys.* **1973**, *2*, 41–51.
- [49] J. P. Perdew, K. Burke, M. Ernzerhof, *Phys. Rev. Lett.* **1996**, *77*, 3865–3868.
- [50] S. Grimme, J. Antony, S. Ehrlich, H. Krieg, *J. Chem. Phys.* **2010**, *132*, 154104.
- [51] A. D. Becke, *J. Chem. Phys.* **1993**, *98*, 1372; A. D. Becke, *J. Chem. Phys.* **1993**, *98*, 5648.
- [52] P. J. Stephens, F. J. Devlin, C. F. Chabalowski, M. J. Frisch, *J. Phys. Chem.* **1994**, *98*, 11623–11627.
- [53] H. Lim, J. Jung, Y. Kim, *Adv. Mater. Interfaces* **2014**, *1*, 1300080.
- [54] R. He, L. Zhao, N. Petrone, K. S. Kim, M. Roth, J. Hone, P. Kim, A. Pasupathy, A. Pinczuk, *Nano Lett.* **2012**, *12*, 2408–2413.
- [55] The image also shows a shift after three molecules at one point. This is due to the presence of an impurity, that is, a NC-Ph₂CN molecule. The assembly compensated for this impurity by locally altering the structure, i.e., already shifting after three molecules.
- [56] C. Kendrick, A. Kahn, *Appl. Surf. Sci.* **1998**, *123/124*, 405–4011.
- [57] J. J. Cox, T. S. Jones, *Surf. Sci.* **2000**, *457*, 311–318.
- [58] R. Hiesgen, M. Rabisch, H. Böttcher, D. Meissner, *Sol. Energy Mater. Sol. Cells* **2000**, *61*, 73–85.
- [59] M. Matena, M. Stöhr, T. Riehm, J. Björk, S. Martens, M. S. Dyer, M. Persson, J. Lobo-Checa, K. Müller, M. Enache, H. Wadepohl, J. Zegenhagen, T. A. Jung, L. H. Gade, *Chem. Eur. J.* **2010**, *16*, 2079–2091.

Manuscript received: December 20, 2018

Accepted manuscript online: January 18, 2019

Version of record online: March 12, 2019